

1 Fine-Mapping and Credible Set Construction using a Multi-

2 population Joint Analysis of Marginal Summary Statistics

3 from Genome-wide Association Studies

4 Jiayi Shen¹, Lai Jiang¹, Kan Wang¹, Anqi Wang², Fei Chen², Paul J. Newcombe³,
5 Christopher A. Haiman^{2,4}, David V. Conti^{1, 2, 4, *}

6 Abstract

7 Recent advancement in Genome-wide Association Studies (GWAS) comes from
8 not only increasingly larger sample sizes but also the shifted focus towards
9 underrepresented populations. Multi-population GWAS may increase power to detect
10 novel risk variants and improve fine-mapping resolution by leveraging evidence from
11 diverse populations and accounting for the difference in linkage disequilibrium (LD)
12 across ethnic groups. Here, we expand upon our previous approach for single-
13 population fine-mapping through Joint Analysis of Marginal SNP Effects (JAM) to a
14 multi-population analysis (mJAM). Under the assumption that true causal variants are

¹ Division of Biostatistics, Department of Population and Public Health Sciences, Keck School of Medicine, University of Southern California, Los Angeles, California, 90032, USA

² Center for Genetic Epidemiology, Keck School of Medicine, University of Southern California, Los Angeles, California, 90033, USA

³ MRC Biostatistics Unit, University of Cambridge, Cambridge, CB2 0SR, United Kingdom

⁴ Norris Comprehensive Cancer Center, University of Southern California, Los Angeles, California, 90033, USA

*Correspondence: dconti@med.usc.edu

15 common across studies, we implement a novel version of JAM that conditions on
16 multiple SNPs while explicitly incorporating the different LD structures across
17 populations. The mJAM framework can be used to first select index variants using the
18 mJAM likelihood with any feature selection approach. In addition, we present a novel
19 approach leveraging the ideas of mediation to construct credible sets for these index
20 variants. Construction of such credible sets can be performed given any existing index
21 variants. We illustrate the implementation of the mJAM likelihood through two
22 implementations: mJAM-SuSiE (a Bayesian approach) and mJAM-Forward selection.
23 Through simulation studies based on realistic effect sizes and levels of LD, we
24 demonstrated that mJAM performs better than other existing multi-ethnic methods for
25 constructing concise credible sets that include the underlying causal variants. In real
26 data examples taken from the most recent multi-population prostate cancer GWAS, we
27 showed several practical advantages of mJAM over other existing methods.

28 Introduction

29 The development of high-throughput genotyping and genotype imputation has
30 boosted the application of genome-wide association studies (GWAS) which is now a
31 standard approach to identify susceptibility loci or genomic regions for many complex
32 diseases and traits^{1,2}. However, the linkage disequilibrium (LD) of single-nucleotide
33 polymorphisms (SNPs) makes it challenging to determine the true causal variant(s)
34 within a region or to further prioritize genetic variants for functional studies^{2,3}.

35 Fine-mapping is a post-GWAS approach which seeks to specify the underlying
36 causal variant and quantify the strength of effect given existing evidence that a certain
37 region is likely to contain at least one causal signal. Many methods for fine-mapping
38 often start with a lead SNP – the SNP with the smallest *p*-value within one region – and
39 then they examine additional highly correlated neighboring SNPs in the region using
40 different strategies such as setting a threshold on pairwise correlation (r^2) with the lead
41 SNP². These approaches are intuitive but do not jointly analyze all the SNPs within a
42 region. In addition, they often do not generalize easily to the investigation in multiple
43 populations.

44 More recent and advanced fine-mapping approaches attempt to jointly or
45 conditionally analyze all SNPs within a region, and include stepwise regression²,
46 penalized regression⁴⁻⁷, and Bayesian methods⁸⁻¹¹. Conditional step-wise selection has
47 been used to discover multiple signals at a locus with individual level data^{12,13}. However,
48 stepwise selection can be very unstable with a large amount of highly correlated SNPs
49 and the *P*-values of the signals in the final selected model tend to be conservative².

50 Alternative selection approaches with individual level data are penalized regression
51 models, such as lasso⁴ and elastic net⁵, and Bayesian methods, such as CAVIAR¹⁰ and
52 Sum of Single Effect models (SuSiE)¹¹. In contrast to step-wise selection, penalized
53 regression techniques are potentially more stable because the penalty term encourages
54 shrinkage of effect estimates towards zero resulting in sparsity and robust estimation.
55 However, penalized often do not perform well with highly correlated SNPs and they do
56 not represent the uncertainty in effect estimation and model selection². In contrast, fully
57 Bayesian methods compute posterior probabilities for models within the model space to
58 infer the probability of causality for each SNP and often result in credible sets to
59 measure the fine-mapping resolution using these probabilities. Ideally, exact inference
60 is possible by enumerating all possible models or combinations of SNPs but the model
61 space increases so rapidly that exhaustive searches become impractical as the number
62 of SNPs increases. Stochastic search algorithms are often used to perform inference on
63 posterior distributions. For example, piMASS⁸ and BVS^{14,15} both use Markov chain
64 Monte Carlo (MCMC) algorithm to search through the model space, while the later can
65 also incorporate external annotations as prior information in the Bayesian model
66 selection to further prioritize causal SNPs.

67 In addition to analyses performed on individual-level data, methods for fine-
68 mapping using only summary statistics from GWAS are becoming more widely applied
69¹⁶⁻¹⁹. In general, these methods use reference samples to estimate the correlations
70 between SNPs and then integrate the correlation structure with modified marginal SNP
71 summary statistics in a multivariable regression framework to approximate the
72 corresponding individual-level analysis. Differences between methods are due to

73 variations in the assumptions for residual error and algorithms for model selection¹⁶⁻¹⁹.
74 For example, FINEMAP¹⁶ places a Gaussian prior for causal effect estimates and
75 adopts a shotgun stochastic search algorithm to prioritize the search to a set of most
76 likely important causal configurations. The original implementation of the Joint Analysis
77 of Marginal SNP Effects (JAM)¹⁹ invokes a Cholesky transformation on the linear
78 regression likelihood, adopts a *g*-prior for effect estimates, and then implements a
79 computationally efficient reversible jump MCMC stochastic search algorithm.

80 Leveraging the information across multiple ethnic groups or ancestry populations
81 can enhance the power of fine-mapping²⁰⁻²². Different ancestry groups may have
82 distinct LD structures due to different evolutionary and migration histories^{23,24}. For
83 example, compared to non-African Americans, African Americans have smaller LD
84 blocks with weaker correlations as the number of recombination events for each region
85 is expected to be higher²⁵. If a true causal variant exists across populations, its
86 corresponding estimated association across populations should be more consistent
87 than the estimated association for proxy SNPs with different LD across populations²⁶⁻²⁸.
88 Therefore, integrating the difference in the LD structures across populations can
89 potentially narrow the credible set that a causal variant resides in and improve the
90 resolution of the fine-mapping^{29,30}.

91 Here, we present an extension of the single-population fine-mapping through
92 JAM to a multi-population setting by fitting a multi-SNP joint model, “mJAM”. mJAM
93 assumes that the true causal variant(s) share the same effect across ancestry groups
94 and it explicitly accounts for different LD structures across ancestry groups in the joint
95 model. The mJAM likelihood allows for different feature selection procedures to be

96 performed on summary statistics obtained from multiple populations. This includes
97 Bayesian variable selection approaches that also yield credible sets or more
98 conventional approaches for only selecting certain SNPs. When combined with
99 approaches that only select specific SNPs, mJAM conditional models can further be
100 used in a mediation type framework to construct credible sets for these index variants in
101 a multi-population analysis. We illustrate this flexibility with two computationally efficient
102 implementations of mJAM: “mJAM-SuSiE” for Bayesian variable selection with native
103 SuSiE credible sets, and “mJAM-Forward” for frequentist forward selection of index
104 SNPs and subsequent credible set construction. Through simulation studies with
105 realistic effect size and various patterns of LD, we compare mJAM-SuSiE and mJAM-
106 Forward with other multi-population approaches, including the most commonly used
107 fixed-effect meta-analysis, COJO¹⁷ with pooled LD structure and meta-analyzed
108 summary statistics, and MsCAVIAR³¹, a Bayesian fine-mapping approach that allows for
109 an arbitrary number of causal variants in a region. We then applied these methods to
110 three known regions for prostate cancer to demonstrate the practical advantages of
111 mJAM.

112 **Material and methods**

113 ***Multi-population JAM***

114 To simplify notation and without loss of generality, we consider the scenario with
115 three populations. Within each population and for a given set of p SNPs within each
116 region, a linear phenotypic model is used.

$$\mathbf{y}^{(i)} = \mathbf{G}^{(i)} \boldsymbol{\beta}_{global} + \epsilon, \text{ for } i = 1, 2, 3 \quad (1)$$

117 where $\mathbf{y}^{(i)}$ is a $N^{(i)} \times 1$ vector of mean-centered phenotypic trait values for the i^{th}
 118 population, with $N^{(i)}$ being the sample size of the i^{th} population; $\mathbf{G}^{(i)}$ is a $N^{(i)} \times p$ matrix
 119 of individual-level genotype data for the i^{th} group, where each SNP has been centered
 120 to its mean; $\boldsymbol{\beta}_{global} \in \mathbb{R}^P$ denotes the joint effect of the given set of p SNPs. $\epsilon \sim N(0, \sigma^2)$
 121 where σ^2 is the residual variance. It is assumed that all three populations share the
 122 same joint effect size, i.e., $\boldsymbol{\beta}_{global}$, and the same residual variance.

123 Akin to a meta-regression, a second-stage model describes the relationship
 124 between the population joint effect estimates and the underlying true effect:

$$\begin{pmatrix} \hat{\boldsymbol{\beta}}^{(1)} \\ \hat{\boldsymbol{\beta}}^{(2)} \\ \hat{\boldsymbol{\beta}}^{(3)} \end{pmatrix} = \begin{pmatrix} \mathbf{I}_P \\ \mathbf{I}_P \\ \mathbf{I}_P \end{pmatrix} \boldsymbol{\beta}_{global} + \delta \quad (2)$$

125 where $\delta \sim N(0, \tau^2)$ and $\hat{\boldsymbol{\beta}}^{(i)} \in \mathbb{R}^P$ is the vector of estimated joint SNP effects for the i^{th}
 126 population.

127 Equation (1) and (2) together form a two-stage model when individual-level
 128 data are available. The first stage is three separate linear phenotypic models whereas
 129 the second stage fits a fixed-effect meta-analysis model that combines all populations
 130 together. By replacing the $\boldsymbol{\beta}_{global}$'s in (1) with (2), we have the following linear fixed-
 131 effect model that incorporates the individual-level data of all populations:

$$\begin{pmatrix} \mathbf{y}^{(1)} \\ \mathbf{y}^{(2)} \\ \mathbf{y}^{(3)} \end{pmatrix} = \begin{pmatrix} \mathbf{G}^{(1)} & 0 & 0 \\ 0 & \mathbf{G}^{(2)} & 0 \\ 0 & 0 & \mathbf{G}^{(3)} \end{pmatrix} \begin{pmatrix} \mathbf{I}_P \\ \mathbf{I}_P \\ \mathbf{I}_P \end{pmatrix} \boldsymbol{\beta}_{global} + \epsilon' \quad (3)$$

132

133 With summary data in which only the marginal effect sizes and their standard errors are
134 available, it is also possible to estimate the joint effect size, β_{global} , with an additional
135 reference sample that estimates the LD between the SNPs^{2,32}. Thus, Equation (3) can
136 be used with only GWAS summary statistics with a modified mJAM likelihood after
137 linear transformation:

$$\mathbf{G}_c \mathbf{I}_c \mathbf{y}_c \sim MVN \left(\left((\mathbf{G}_c \mathbf{I}_c)' \mathbf{G}_c \mathbf{I}_c \right) \beta_{global}, \sigma^2 \left((\mathbf{G}_c \mathbf{I}_c)' \mathbf{G}_c \mathbf{I}_c \right) \right) \quad (4)$$

138 where $\mathbf{G}_c, \mathbf{y}_c, \mathbf{I}_c$ denotes $\begin{pmatrix} \mathbf{G}^{(1)} & \mathbf{0} & \mathbf{0} \\ \mathbf{0} & \mathbf{G}^{(2)} & \mathbf{0} \\ \mathbf{0} & \mathbf{0} & \mathbf{G}^{(3)} \end{pmatrix}$, $\begin{pmatrix} \mathbf{y}^{(1)} \\ \mathbf{y}^{(2)} \\ \mathbf{y}^{(3)} \end{pmatrix}$ and $\begin{pmatrix} \mathbf{I}_P \\ \mathbf{I}_P \\ \mathbf{I}_P \end{pmatrix}$ in Equation (3)

139 respectively. By expanding each matrix, we have $\mathbf{G}_c \mathbf{I}_c \mathbf{y}_c = \sum_{i=1}^3 \mathbf{G}^{(i)'} \mathbf{y}^{(i)}$ and
140 $(\mathbf{G}_c \mathbf{I}_c)' \mathbf{G}_c \mathbf{I}_c = \sum_{i=1}^3 \mathbf{G}^{(i)'} \mathbf{G}^{(i)}$ where $\mathbf{G}^{(i)'} \mathbf{G}^{(i)}$ and $\mathbf{G}^{(i)'} \mathbf{y}^{(i)}$ are population-specific
141 statistics and can be estimated by population-specific GWAS summary statistics and a
142 reference genotype matrix or LD matrix. Detailed derivation can be found in
143 Supplemental Methods.

144 ***Index SNP Selection and Credible Set Construction for Fine Mapping***

145 mJAM establishes a multi-SNP model within each population with corresponding
146 population-specific LD, while jointly estimating a fixed-effects summary estimate of
147 effect. The mJAM likelihood presented in Equation (4) can be used in a wide variety of
148 existing feature selection approaches which are applicable to the mJAM statistics
149 shown in Equation (4). Possible approaches for index SNP selection in mJAM includes
150 stepwise selection², Ridge regression⁷, and Bayesian approaches such as SuSiE¹¹.

151 We adopt a forward selection approach based on conditional P -value for index
152 SNP selection because of its computational efficiency and straightforward interpretation.
153 We define our implementation of “mJAM-Forward” as a two-step approach in which a
154 first step relies on a conventional stepwise forward selection to select an additional
155 index SNP based on its corresponding P -value from a mJAM model conditional on any
156 previous index SNP(s). We incorporate a g -prior to stabilize effect estimates³³. To avoid
157 fitting models with highly correlated SNPs we include a pruning process within Algorithm
158 1.

159 The second step for mJAM-Froward is to define a multi-population credible set
160 for each index SNP. Here, we fit two mJAM models for each candidate credible set
161 SNP, W , located within a region of an index SNP, X . These models demonstrate that
162 the candidate credible set SNP is: 1) associated with disease marginally, and 2) that the
163 index SNP mediates the effect of the candidate SNP on the disease. The first model
164 includes W by itself to yield a probability that W is associated with the trait. This model
165 also provides a posterior distribution for the marginal effect for the candidate credible
166 set SNP.

$$Pr(M_W | Data) = \frac{p(M_W)BF[M_W : M_{Null}]}{\sum_w p(M_w)BF[M_w : M_{Null}]} \quad (5)$$

167 where $p(M_W)$ is the prior density of one-SNP model that includes W and $BF[M_W : M_{Null}]$
168 is the Bayes factor of one-SNP model with W to the null model. See Supplemental
169 Methods for detailed expression of $BF[M_W : M_{Null}]$ with the incorporation of a g -prior of
170 the effect estimates. The second model conditions on the index SNP, X , to obtain a
171 posterior estimate for an adjusted effect estimate for the credible set SNP. Borrowing

172 from a mediation framework³⁴, we then calculate the probability that the index SNP
173 mediates the candidate credible set SNP effect using the two models (Figure 1).

$$Pr(Mediation|Data) = Pr(|\tau_W - \tau'_W| > 0|Data) \quad (6)$$

174 where τ_W is the total effect of the candidate credible set SNP on the outcome and τ'_W is
175 the direct effect. A strong mediation effect indicates that the observed marginal effect of
176 the candidate credible set SNP on the outcome is mainly due to its indirect effect
177 through its strong correlation with the index SNP, and not due to a direct effect on the
178 outcome. These two model probabilities are then combined to calculate the probability
179 that a candidate SNP is a credible set SNP, Posterior Credible Set Probability (PCSP).

$$PCSP_W := Pr(M_W | Data) \cdot Pr(|\tau_W - \tau'_W| > 0|Data) \quad (7)$$

180 PCSP are then scaled over all SNPs in the region and used to define a 95% credible set
181 of cross-population SNPs.

182 **Algorithm 1 Pseudo algorithm for fitting mJAM-Forward and credible set
183 construction in a region**

Input data: $\hat{\beta}^{(i)}$, $se(\hat{\beta}^{(i)})$, sample size of GWAS N_{GWAS} , Effect Allele Frequencies
 $EAF^{(i)}$, $G_R^{(i)}$ for each study indexed by i

Input arguments: LD threshold for index SNP selection, conditional P -value threshold

1. Compute mJAM statistics $(G_c I_c)' G_c I_c$, $(G_c I_c)' y_c$, and $y_c' y_c$
2. Compute marginal mJAM P -values under g prior specification for all testing SNPs in the region
3. While the smallest conditional P -value (or marginal P -value in the first round only) is smaller than threshold:
4. Identify the testing SNP with the smallest conditional P -value as the next index SNP
5. Construct credible set of the new index SNP
6. Prune out SNPs in LD with the new index SNP based on LD threshold

7. Compute the conditional mJAM P -value for all remaining SNPs in the region
8. Stop until no SNP in the region has conditional P -value smaller than threshold

Return index SNP(s), corresponding conditional P -value(s) and credible set(s).

184 We also integrate the mJAM likelihood and summary statistics into a Bayesian
185 selection method that indicates index SNPs and simultaneously estimates credible set
186 SNPs, “mJAM-SuSiE” (See Supplemental Methods for the pseudo-algorithm of fitting
187 mJAM-SuSiE)³⁵.

188 ***Incorporating missing variants in mJAM***

189 In genetic association studies with more than one cohort or study, it is common
190 that a particular SNP might be available in some studies but missing in the others³⁶. A
191 notable practical feature of the mJAM framework is that it allows for these SNPs with
192 missing information to be analyzed without being filtered or removed. This is
193 accomplished with a simple modification by substituting a value of zero in the identity
194 matrix in Equation (3) and (4). Such modification then allows for observed statistics
195 from other populations to be used but removes the contribution from the population in
196 which it is missing but does not alter the algorithm nor the fitting process. This
197 modification is applicable either when the SNP is missing in the reference panel or
198 when the population-specific GWAS summary statistics are not available for the SNP
199 (See Supplemental Methods for more details).

200 ***Simulation Study on Structured LD***

201 We conducted a simulation study to compare the performance of the two mJAM
202 implementations (mJAM-SuSiE and mJAM-Forward) with three commonly used

203 alternative approaches: fixed-effect meta-analysis, COJO stepwise selection and
204 MsCAVIAR. Fixed-effect meta-analysis takes an inverse-variance weighted average of
205 the marginal estimates from individual studies or populations. COJO approximates the
206 conditional and joint effect from summary statistics and single reference LD and then
207 implements a stepwise selection based on conditional *P*-values. Additionally, for use of
208 COJO on multiple populations, the summary-level statistics come from the fixed-effect
209 meta-analysis across all populations and the reference LD can be obtained from either
210 the pooled individual-level genotype data or a subset of meta-analysis sample. We used
211 the former as the reference LD for COJO in our simulations. MsCAVIAR is built upon a
212 Bayesian multivariate normal framework first described as CAVIAR¹⁰ to account for
213 between-study or between-population heterogeneity using a random-effects model. To
214 compare the performance of index SNP selection across these multi-population
215 approaches, we use three metrics: number of selected index SNPs, sensitivity/power,
216 and positive predictive value (PPV). In addition, since MsCAVIAR, mJAM-SuSiE, and
217 mJAM-Forward output credible set(s) within each region, we compare credible set
218 performance using the number of credible set(s), size of each credible set,
219 sensitivity/power, PPV and empirical coverage. For the two non-Bayesian methods, FE
220 and COJO, we consider the group of SNPs with meta-analyzed or conditional *P*-values
221 less than a Bonferroni-corrected significance level as a single credible set for the
222 purpose of performance comparison.

223 We performed two sets of scenarios: 1) simulated correlation structures with the
224 same block LD structures across populations; and 2) simulated correlation based on
225 real genetic correlation structures observed in the study cohort from Elucidating Loci

226 Involved in Prostate Cancer Susceptibility (ELLIPSE) OncoArray Consortium²¹. For the
227 first set of scenarios, we first simulated a baseline scenario where each population has
228 3 individual association studies with $N = 5,000$ each to closely represent the real-life
229 situation where there are multiple association studies performed for each ethnic group
230 (total sample size = $5,000 \times 3$ studies/population $\times 3$ population = 45,000). A total of 50
231 SNPs are simulated in 5 blocks of 10 SNPs. Within each block of 10 SNPs, the pair-
232 wise correlations are uniformly set to a constant value r^2 across ancestries for simplicity.
233 r^2 varies from 0, 0.6² and 0.9² to represent independent, moderate LD and high LD
234 scenarios. Corresponding LD heatmaps are shown in Figure S1. We then selected a
235 single causal SNP with an effect size of 0.03 for a standard normal outcome. The
236 baseline scenario was extended by varying parameters, including the ratio of sample
237 sizes between each population, levels of LD, the total number of causal SNPs and
238 corresponding effect sizes.

239 ***Simulation Study with Real Data***

240 To better capture realistic LD patterns, we performed simulations based on real
241 correlation within three ancestry groups (Europeans, African Americans, and East
242 Asians) from the ELLIPSE OncoArray Consortium²¹. The available sample sizes for
243 these three populations are 93,749 Europeans, 9,531 African Americans, and 2,075
244 Asians. We simulated 120 SNPs within a 1334 kb region from chromosome 2 using a
245 multivariate normal model with an estimated correlation structure from individual-level
246 genotypes. The heatmap of this region for each ethnicity is shown in Figure S2. In each
247 simulation, we randomly chose one SNP out of a selected LD block to be the causal
248 SNP with effect size being 0.04, resulting in an empirical average $-\log_{10}(P\text{-value})$ of the

249 most significance variant of 7.75 (P -value $\approx 1.8 \times 10^{-8}$) averaged across 500
250 simulations.

251 ***Applied examples***

252 To illustrate mJAM on real data, we applied the methods on three regions using
253 summary statistics from the latest cross-ancestry prostate cancer association study³⁷
254 across four ancestry groups, including 122,188 prostate cancer cases and 604,640
255 controls of European ancestry, 19,391 cases and 61,608 controls of African ancestry,
256 10,809 cases and 95,790 controls of East Asian ancestry, and 3,931 cases and 26,405
257 controls from Hispanic populations. Within each region, we applied mJAM-Forward to
258 select index SNP(s) using population-specific summary statistics and reference dosage
259 for each population. Then we constructed mJAM credible set(s) by including top SNPs
260 ranked by their mJAM posterior probabilities until those SNPs included in the credible
261 set reached a cumulative posterior probability of 95%. Reference dosage were obtained
262 from the Prostate Cancer Association Group to Investigate Cancer-Associated
263 Alterations in the Genome and Collaborative Oncological Gene-Environment Study
264 Consortium [PRACTICAL iCOGS], the Elucidating Loci Involved in Prostate Cancer
265 Susceptibility OncoArray Consortium [ELLIPSE OncoArray], the African Ancestry
266 Prostate Cancer Consortium [AAPC GWAS], GWAS of prostate cancer in Latinos
267 [LAPC GWAS] and Japanese [JAPC GWAS]²¹. Results from mJAM-Forward are
268 compared with those from mJAM-SuSiE, COJO and MsCAVIAR.

269 Results

270 ***Simulation Study on Artificial LD***

271 Under the baseline scenario (50 SNPs in total, 1 causal SNP with an effect size
272 of 0.03, 3 studies per population, and balanced sample size across populations), the
273 95% credible sets from mJAM-Forward, mJAM-SuSiE, and MsCAVIAR were well
274 calibrated to the specified coverage level (Figure S3). Both mJAM-Forward and mJAM-
275 SuSiE preserved relatively high sensitivity in terms of including the true causal SNP in
276 its credible set (sensitivity = 0.86 and 0.64 respectively, Figure 2A). Although
277 MsCAVIAR had the highest sensitivity (0.99) under the baseline scenario, its average
278 credible set size was much larger (9.47 for MsCAVIAR; 2.12 for mJAM-Forward and
279 0.78 for mJAM-SuSiE, Figure 2C), thus leading to a much lower PPV (0.39, Figure 2B).
280 mJAM-SuSiE had the highest PPV (0.89) among the methods we compared, meaning
281 that it had the highest proportion of true causal over the total number of credible set
282 SNPs on average, followed by mJAM-Forward (0.58) (Figure 2B). In terms of credible
283 set sensitivity, PPV and average CS size the methods had similar patterns of
284 performance for scenarios expanded beyond the baseline to various LD structures,
285 imbalanced sample size across populations, and 3 causal SNPs (Figure S4).

286 In terms of identifying the true causal variant as an index SNP (i.e. sensitivity),
287 mJAM-Forward and MsCAVIAR had the best performance under moderate LD
288 scenarios (Figure 3A) with a sensitivity was 0.73, and 0.72 respectively. However, for
289 these two methods, mJAM-Forward had a better PPV was 0.81, compared to
290 MsCAVIAR (0.72). In comparison, mJAM-SuSiE had poor sensitivity (0.62) but a higher

291 PPV (0.88). COJO had a similar performance with mJAM-Forward under independent
292 LD scenarios but its sensitivity and PPV worsened compared to mJAM-Forward as the
293 level of LD increases. Though COJO performs a similar stepwise selection as mJAM-
294 Forward, unlike mJAM-Forward that specifically accounted for population-specific LD,
295 COJO uses meta-analyzed marginal summary statistics and pooled LD panel which
296 makes it difficult to identify the true common variants through disentangling the
297 population-specific LD structure. All methods selected on average 1 index SNP among
298 500 simulations, close to the true number of causals (Figure 3C). For MsCAVIAR pre-
299 specification is required so we set the value to 1 for all scenarios. Notably for practical
300 implementation, for a small number of scenarios (40%), mJAM-SuSiE did not select any
301 index SNP under independent or moderate LD scenarios, leading to relatively low
302 sensitivity compared other methods when averaged over replicates (Figure 3A).

303 When the pairwise correlation within each LD block increased, the average
304 credible set sizes for all methods increased correspondingly (Figure 2C). As a result,
305 under high LD scenarios, the PPV of identifying the true causal(s) in a credible set
306 decreased to a noticeable extent for MsCAVIAR, mJAM-Forward, and FE (Figure 2B).
307 Though mJAM-Forward's PPV dropped due to the increase in credible set sizes on
308 average, mJAM-Forward was still able to retain a sensitivity of 0.88 under the high LD
309 scenario. mJAM-SuSiE achieved the highest PPV (0.81, Figure 2B) among all methods
310 under high LD scenarios while retaining relatively high sensitivity and small credible set
311 size. However, mJAM-SuSiE's sensitivity was relatively low compared to mJAM-
312 Forward and MsCAVIAR under independent or moderate LD scenarios (Figure 2A).

313 Despite of mJAM-SuSiE's outstanding performance under high LD scenarios with
314 moderate causal effect size, we noticed that its results were very sensitive to the
315 marginal significance of the true causal SNPs. To represent a real-life situation where a
316 lead variant within a region has an extremely significant marginal *P*-value, we expanded
317 the baseline scenario with 1 true causal SNP to additional scenarios with increasing
318 significance of the true causal SNP, where the average $-\log_{10}(P\text{-value})$ of the true
319 causal ranges from 5 to 263 (mimicking significance often found in applied GWAS).
320 Under increasingly high-power scenarios, mJAM-Forward consistently selected 1
321 credible set regardless of the significance of the true causal whereas the average
322 number of credible sets by mJAM-SuSiE increased as the statistical significance (i.e.
323 effective power) increased (Figure 4B). As a result, mJAM-SuSiE selected more false
324 positive SNPs within the credible sets when the true causal SNP has high observed
325 marginal significance. In addition, the empirical coverage of mJAM-SuSiE's credible
326 sets dropped below the expected level quickly after the true causal SNP became more
327 significant (Figure 4A). In contrast, mJAM-Forward's credible sets remained well-
328 calibrated.

329 To explore the impact of two types of missingness on the performance of mJAM-
330 Forward, we modified our simulation studies with artificial LD structure to include a
331 missing SNP in LD with the causal SNP, or with the missing SNP as the causal SNP
332 itself. The flexibility of mJAM likelihood (Equation 2) allows us to incorporate SNPs with
333 missing information in some studies or populations in the analysis. We found that when
334 the missing SNP is in LD with the causal SNP, mJAM-Forward has stable performance
335 in comparison to when there is no missingness (Figure S6). When the causal SNP is

336 missing, mJAM-Forward still preserves the power both to select the causal SNP as the
337 index SNP and to include the causal SNP in its credible set.

338 ***Simulation Study on Real LD***

339 When applied to the simulated data on the 120-SNP region on chromosome 2,
340 mJAM-Forward, mJAM-SuSiE and MsCAVIAR selected on average around 1 index
341 SNP whereas COJO selected 1.5 index SNPs, indicating a slight increase in false
342 positive signals. mJAM-Forward had highest sensitivity and PPV of identifying the true
343 causal from a complicated LD structure as an index SNP (Table 1). In terms of credible
344 set performance, MsCAVIAR demonstrated high empirical coverage of its credible set
345 as well as high sensitivity compared to the other two mJAM methods. However, such
346 high sensitivity and PPV was achieved at the cost of a much larger size for the credible
347 sets. The average size of the 95% CS of MsCAVIAR is 56.52, even larger than the
348 number of SNPs that reached marginal genome-wide significant (5×10^{-8}) in a fixed-
349 effect meta-analysis (48.88). On the other hand, the average credible set size for
350 mJAM-Forward and mJAM-SuSiE was 19.70 and 18.37 respectively. Meanwhile, both
351 approaches preserved reasonably high sensitivity and empirical coverage.

352 ***Applied example 1: a single-hit region on chromosome 12***

353 The first applied example is a 1013 kb region on chromosome 12 which consists
354 of 276 SNPs with a marginal meta-analyzed P -value $< 10^{-3}$ and minor allele frequency
355 (MAF) $> 2\%$. Figure S7 shows the LD structure for the four ancestry groups in this
356 analysis. None of the SNPs in this region reached genome-wide significance in any
357 population-specific analyses (Figure 5B) but after multi-population meta-analysis 48

358 SNPs are genome-wide significant (Figure 5A). By setting a conditional *P*-value
359 threshold at 5×10^{-8} , mJAM-Forward identified one index SNP at 12:109994870:A:T
360 (meta *P*-value = 3.5×10^{-10}) with a corresponding 95% credible set of 41 SNPs. The
361 median r^2 between the credible set SNPs with the index SNP is 0.998 for European LD,
362 0.979 for African, 0.990 for Hispanic and 0.996 for East Asian. COJO identified the
363 same index SNP, 12:109994870:A:T. MsCAVIAR reported a slightly larger 95% credible
364 set than mJAM-Forward, consisting of 45 SNPs (Figure S8). The index SNP of
365 MsCAVIAR's credible set is 12:109998097:A:G (meta *P*-value = 3.7×10^{-10}) whose r^2
366 with 12:109994870:A:T is greater than 0.99 in all four ancestry groups. This index SNP,
367 12:109998097:A:G, is included in a mJAM-Forward credible set only when coverage is
368 increased to 99%; whereas the index SNP for mJAM-Forward, 12:109994870:A:T, is
369 included in the 95% MsCAVIAR credible set. mJAM-SuSiE estimates a single 95%
370 credible set with 28 total SNPs and a unique single index SNP, 12:109996343:A:C
371 (meta *P*-value = 2.2×10^{-9}) which is also included in both credible sets of mJAM-
372 Forward and MsCAVIAR. The median r^2 within a credible set is also greater than 0.99
373 for all ancestry groups (Table S1). The index SNP from mJAM-Forward was also
374 included in its credible set (Figure S8B).

375 ***Applied example 2: Asian-driven signals on chromosome 10***

376 As a second example, we conducted an analysis on a chromosome 10 region
377 which consists of 412 SNPs after QC and spans around 1571 kb. Figure S9 shows the
378 LD structure in this region separately for European, African, East Asian, and Hispanic
379 populations. This region contains two clear signals with meta-analyzed *P*-value $< 10^{-15}$,
380 which are mainly driven by the results from East Asian and African populations (Figure

381 6). In this example, mJAM-Forward identified two index SNPs, 10:80835998:C:T (meta
382 P -value = 9×10^{-21} and 10:80238015:C:T (meta P -value = 1×10^{-19}) (Figure 6A). The
383 95% mJAM-Forward credible set for the first index SNP, 10:80835998:C:T, contains 3
384 SNPs in total and there are 45 SNPs in the credible set for the second index SNP. The
385 minimum r^2 between the mJAM-Forward credible set SNPs with its own index SNP is no
386 less than 0.95 in European, East Asian and Hispanic populations, and no less than 0.81
387 in African ancestry populations (Table S2). COJO identified two index SNPs,
388 10:80835998:C:T and 10:80240493:A:G. 10:80835998:C:T is the same as one of the
389 index SNPs selected by mJAM-Forward and 10:80240493:A:G is included in the mJAM-
390 Forward 95% credible set of 10:80238015:C:T. Since MsCAVIAR does not support
391 reporting more than one distinctive credible set, we split this region into two adjacent
392 regions and applied MaCAVIAR on these two subregions separately. MsCAVIAR
393 selected the same 3-SNP 95% credible set (Figure S10) with index SNP being
394 10:80835998:C:T, and another 45-SNP credible set with index SNP being
395 10:80238015:C:T where 42 of them are replicated in the mJAM-Forward credible set.
396 mJAM-SuSiE also identified the same 3-SNP credible set (95%) with the same index
397 SNP 10:80835998:C:T but did not identify any credible set around 10:80238015:C:T.
398 Instead, it reported two additional credible sets at 10:80260938:V1 (meta P -value =
399 2×10^{-10}) and 10:80476778:V1 (meta P -value = 4×10^{-4}) (Figure S10), and the
400 credible set size is 2 and 5 respectively.

401 **Applied example 3: Secondary signal within 40kb region of a leading SNP**

402 The third applied example illustrates a scenario where there is a secondary
403 signal within close proximity of the leading SNP in a chromosome 11 region. This region

404 spans 335.5 kb and consists of 191 SNPs that passed QC. The population-specific LD
405 structure and Manhattan plot of multi-population meta-analysis results are shown in
406 Figure S11 and Figure 7. The lead variant, 11:102401661:C:T, has a multi-population
407 meta-analyzed *P*-value of 1.5×10^{-38} and mJAM-Forward identified a secondary index
408 SNP, 11:102440927:A:G, only 39 kb away which has a meta *P*-value of 4.9×10^{-11} .
409 The r^2 between these two index SNPs is less than 0.01 in all four ancestry groups
410 (Figure S11), suggesting statistical independence between these two SNPs. COJO
411 selected the same primary index SNP, 11:102401661:C:T, and a different secondary
412 index, 11:102433309:A:G, which has a meta *P*-value of 1.3×10^{-7} and is highly
413 correlated with 11:102440927:A:G ($r^2 = 0.79$ in EUR; 0.55 in AA; 0.87 in LA and 0.99 in
414 ASN). mJAM-SuSiE also selected two credible sets in this region: the first set has 2
415 SNPs which are both replicated in mJAM-Forward's first credible set; the second set
416 has 26 SNPs where 24 of them are found in mJAM-Forward's second set. However, the
417 index SNP of the second set in mJAM-SuSiE is one with lower marginal significance
418 (meta *P*-value = 6.3×10^{-5}) compared to mJAM-Forward.

419 Both mJAM-SuSiE and mJAM-Forward are able to identify multiple sets within
420 one region without any pre-defined number of causal variants. On the other hand, the
421 implementation of MsCAVIAR requires users to specify the maximum number of causal
422 variants in a region to enumerate all possible causal configurations. Gauging the
423 possible number of causal variants can be difficult when secondary signals are located
424 close to the lead variant. In this example, the secondary signal is located only 39 kb
425 away from the leading variant, and visual inspection of the Manhattan plot (Figure 7)
426 suggests only one peak. Even if we specify the number of causal variants to be two

427 when applying MsCAVIAR to this region, MsCAVIAR reports only one credible set such
428 that the posterior probability of this set containing 2 causal variants is at least 0.95.
429 Thus, it becomes difficult to separate the selected credible set SNPs into two distinctive
430 groups. When the number of causal variants is set to two, MsCAVIAR selected 24
431 SNPs among which the 2 SNPs with highest posterior probability are 11:102401661:C:T
432 and 11:102396607:C:T (Figure S12). However, these two SNPs are in high LD and thus
433 are likely linked to a single underlying causal signal and not indicative of multiple
434 independent signals.

435 Discussion

436 As integrating studies from ancestrally diverse populations may increase power
437 to detect novel variant and improve fine-mapping resolution^{22,38,39}, we extend our
438 previous single-population fine-mapping through JAM to a multi-population approach,
439 mJAM. mJAM requires only population-specific summary statistics and population-
440 specific reference LD panels, which are more accessible than individual-level data to
441 many researchers. mJAM explicitly incorporates the different LD structures across
442 populations to yield conditional estimates of SNP effects from a single joint model. The
443 mJAM framework can be used to first select index SNPs using existing feature selection
444 approaches, such as forward stepwise selection², Bayesian model selection^{8,9,11}, or
445 regularized regression^{6,7}. To demonstrate this flexibility, we have implemented mJAM
446 through two implementations of feature selection: mJAM-SuSiE (a Bayesian approach)
447 and mJAM-forward selection. We also combine the forward selection implementation
448 with a second step to identify credible set SNPs. This step works given any set of index

449 SNPs within a region by estimating a posterior credible set probability (PCSP) for a SNP
450 defined as a combination of two component probabilities: one models the marginal
451 association between the candidate SNP and the outcome; the other models the
452 mediation effect of the index SNP on the candidate SNP, borrowing from a mediation
453 framework. These PCSPs are then used to construct credible sets. The closed-formed
454 expression for PCSP allows computational efficient construction of credible sets,
455 compared to other Bayesian approaches that often use computationally intensive
456 algorithms to obtain posterior distributions. It also allows credible set construction from
457 any index SNP list allowing researchers to apply other feature selection methods or use
458 existing lists or knowledge to determine index SNP.

459 The two-stage model framework utilized in mJAM builds upon previous work
460 highlighting the use of hierarchical JAM (hJAM)⁴⁰, an approach for the joint analysis of
461 marginal summary statistics that incorporates a prior information matrix. This matrix
462 characterizes the SNPs and can include information such as SNP effects on gene
463 expression analogous to TWAS or on intermediates biomarkers analogous to Mendelian
464 randomization. mJAM is an extension to hJAM in that it replaces the prior information
465 matrix in hJAM with a stacked identity matrix, $\begin{pmatrix} I_P \\ I_P \\ I_P \end{pmatrix}$, as described in Methods section.
466 The stacked identity matrix can be interpreted as our prior belief on the joint SNP
467 effect estimates that all populations share the same true effect sizes.

468 In a set of realistic simulation settings, both mJAM implementations
469 demonstrated the ability to infer the number of independent signals within a region, to
470 differentiate signals from noise, and to achieve a sufficient level of sensitivity while

471 preserving high fine-mapping resolution through small-sized credible sets. We also
472 investigated the impact of imbalanced sample size across populations on model
473 performance and demonstrated that all methods showed a similar decrease in terms of
474 sensitivity and PPV when the sample size is imbalanced but the total sample size
475 remains constant (Figure S4). mJAM is described using three populations in simulation
476 studies and we apply mJAM to real data with four distinct populations. In practice,
477 mJAM can be used to analyze a large number of studies or population-specific
478 summary statistics facilitating flexibility in application. Thus, analyses do not need to be
479 limited to aggregating continental ancestry populations, but can include numerous, more
480 specific ancestry appropriate reference panels to aggregate data across many studies
481 (Figure S5). However, as with all summary statistic approaches that rely on reference
482 panels, the ability to disentangle highly correlated SNPs will be driven by the sample
483 sizes⁴¹ and LD within and between the reference panels used⁴². In addition, another
484 practical limitation to many summary statistics-based approaches is the requirement for
485 complete summary statistics and reference data for all SNPs across all studies and
486 populations analyzed³⁶. Missingness can be due to the difference in genotyping arrays
487 used by different studies, or rare variants not being captured due to limited sample size
488 in certain studies. Filtering too many variants might be dangerous because as less
489 information is used to disentangle the LD structure within each region and potentially
490 missing the causal variant. An important feature of mJAM is that it will work even in the
491 presence of differential missingness across studies or populations utilizing all
492 information that is available.

493 In the simulation study with artificial LD structures, mJAM-SuSiE resulted in
494 outstanding performance under high LD scenarios, achieving both high sensitivity and
495 high PPV. However, as the significance of the causal variant(s) within a region
496 increases, mJAM-SuSiE tends to break down selecting more false positive signals with
497 each in separate credible sets. This results in a substantial decrease in the empirical
498 coverage of mJAM-SuSiE credible sets. In practice, we recommend limiting the
499 application of mJAM-SuSiE to only regions with SNPs with modest marginal statistically
500 significance or to screen for any potential false positive credible sets before interpreting
501 mJAM-SuSiE's credible sets after estimation.

502 We also carried out a case study of prostate cancer where mJAM is applied to
503 several prostate cancer susceptible regions. Through three different regions with
504 different characteristics in number of estimated independent signals and underlying LD
505 within and between populations, we demonstrated the practical advantages of mJAM-
506 Forward, including allowing more than one causal variant within a region, outputting
507 individual credible sets corresponding to each index, and easily interpretable index
508 variants with conditional estimates. In addition to the three applied examples shown
509 here, mJAM has been applied to perform index variants selection across all regions in
510 the latest multi-population prostate cancer GWAS³⁷ which is currently under review.

511 For all approaches that use marginal summary statistics and reference data,
512 careful consideration and construction of the correlation matrices is important. This
513 includes using a reference panel with ancestry and LD that matches the population in
514 which the original marginal summary statistics were estimated^{41,43}. The methods also
515 require that the correlation matrix used is full rank and positive-definite which is often

516 driven by the sample size of the data and the frequency of the SNPs. For mJAM such
517 consideration must be considered across all populations used in the analysis. Firstly, for
518 rare variants, mJAM estimates of multi-population effect and standard errors that can be
519 different from the marginal meta-analyzed estimates which use inverse-variance
520 weighting. mJAM estimation from summary statistics assume Hardy-Weinberg
521 equilibrium which some variants, especially rare variants, might not satisfy. In addition,
522 many rare variants will also have large effect sizes and large standard errors from the
523 population-specific summary statistics thus resulting in more uncertainty in multi-
524 population analysis compared to variants that are common across all populations.
525 Secondly, in regions with extremely significant lead variants from a well-powered
526 GWAS, even small degrees of LD can pull the marginal and conditional effect estimates
527 of other variants away from the null. Thus, false positive signals might be selected if we
528 apply the same threshold for index SNP selection and LD pruning. For such regions,
529 researchers may consider setting a higher significance threshold for secondary signal
530 selection and a more stringent LD threshold for pruning out correlated signals.

531 In conclusion, mJAM offers a flexible and efficient modeling framework for multi-
532 population fine-mapping that first selects index variants and then constructs credible
533 sets. One key assumption in mJAM is that causal variants and their effect sizes are
534 similar across all populations and there exists evidence suggesting that common causal
535 variants tend to have consistent effect sizes across populations²⁶⁻²⁸. In future research,
536 we plan to relax the current mJAM assumption to allow different true effect sizes across
537 populations. Other potential future directions include follow-up functional analyses
538 based on mJAM credible sets and polygenic risk score models based on mJAM fine-

539 mapped results. mJAM is currently available as a R package for fine-mapping of
540 specific regions and can easily be adapted for genome-wide applications.

541

542 **Tables**

543 **Table 1 Comparison of model performance on data simulated from real LD**

544 **structure.**

		Method				
		mJAM-Forward	mJAM-SuSiE	FE	COJO	MsCAVIAR
Credible Set Performance	Sensitivity ^a	0.930	0.910	0.972	-	0.994
	PPV ^b	0.064	0.069	0.024	-	0.022
	CS size ^c	19.70	18.37	48.88	-	56.62
	CS coverage ^d	0.934	0.940	-	-	1.000
Index SNP Performance	Sensitivity ^e	0.218	0.174	-	0.186	0.134
	PPV ^f	0.219	0.021	-	0.144	0.134
	Number of selected index	1.00	0.97	-	1.51	1.00

545 Abbreviations: FE, fixed-effect meta-analysis; CS, credible set, PPV, positive predictive value.

546 ^a proportion of true causal SNPs being selected in a credible set, averaged over 500 simulations

547 ^b proportion of true causal SNPs over the total number of selected credible set SNPs, averaged over 500 simulations.

549 ^c total number of SNPs included in a credible set, averaged over all 95% credible sets in 500 simulations.

551 ^d proportion of 95% credible sets in 500 simulations that included at least one true causal SNP.

552 ^e proportion of true causal SNPs being selected as an index SNP, averaged over 500 simulations.

553 ^f proportion of true causal SNPs over the total number of selected index SNPs, averaged over 500 simulations.

555

556

557 **Declaration of interests**

558 The authors declare no competing interests.

559 **Acknowledgements**

560 This research was supported by P01CA196569, U01CA261339, P30CA014089,
561 U01CA257328, U19CA214253, and R01HG010297.

562 **Data and code availability**

563 Both mJAM-Forward and mJAM-SuSiE are available as an R package at
564 <https://github.com/USCbiostats/hJAM/R>. The codes used for simulations and real data
565 examples are available at https://github.com/USCbiostats/hJAM/manuscript_codes.

566 **References**

- 567 1. Buniello, A., MacArthur, J.A.L., Cerezo, M., Harris, L.W., Hayhurst, J., Malangone, C., McMahon, A., Morales, J., Mountjoy, E., and Sollis, E. (2019). The NHGRI-EBI GWAS Catalog of published genome-wide association studies, targeted arrays and summary statistics 2019. *Nucleic acids research* 47, D1005-D1012.
- 568 2. Schaid, D.J., Chen, W., and Larson, N.B. (2018). From genome-wide associations to candidate causal variants by statistical fine-mapping. *Nature Reviews Genetics* 19, 491-504.
- 569 3. Visscher, P.M., Brown, M.A., McCarthy, M.I., and Yang, J. (2012). Five years of GWAS discovery. *The American Journal of Human Genetics* 90, 7-24.
- 570 4. Tibshirani, R. (1996). Regression shrinkage and selection via the lasso. *Journal of the Royal Statistical Society: Series B (Methodological)* 58, 267-288.
- 571 5. Cho, S., Kim, H., Oh, S., Kim, K., and Park, T. (2009). Elastic-net regularization approaches for genome-wide association studies of rheumatoid arthritis. *BMC Proceedings* 3, S25. 10.1186/1753-6561-3-s7-s25.
- 572 6. Ayers, K.L., and Cordell, H.J. (2010). SNP Selection in genome-wide and candidate gene studies via penalized logistic regression. *Genetic Epidemiology* 34, 879-891. 10.1002/gepi.20543.
- 573 7. Hastie, T. (2020). Ridge Regularization: An Essential Concept in Data Science. *Technometrics* 62, 426-433. 10.1080/00401706.2020.1791959.
- 574 8. Guan, Y., and Stephens, M. (2011). Bayesian variable selection regression for genome-wide association studies and other large-scale problems. *The Annals of Applied Statistics*, 1780-1815.
- 575 9. Chen, W., Larrabee, B.R., Ovsyannikova, I.G., Kennedy, R.B., Haralambieva, I.H., Poland, G.A., and Schaid, D.J. (2015). Fine Mapping Causal Variants with an Approximate Bayesian Method Using Marginal Test Statistics. *Genetics* 200, 719-736. 10.1534/genetics.115.176107.
- 576 10. Hormozdiari, F., Kostem, E., Kang, E.Y., Pasaniuc, B., and Eskin, E. (2014). Identifying causal variants at loci with multiple signals of association. *Genetics* 198, 497-508. papers3://publication/doi/10.1534/genetics.114.167908.

592 11. Zou, Y., Carbonetto, P., Wang, G., Stephens, M.V.O.P., and Stephens, V.O.P.M. (2022). Fine-
593 mapping from summary data with the “Sum of Single Effects” model. *bioRxiv*.
594 <https://doi.org/10.1101/2021.11.03.467167>.

595 12. Galarneau, G., Palmer, C.D., Sankaran, V.G., Orkin, S.H., Hirschhorn, J.N., and Lettre, G. (2010).
596 Fine-mapping at three loci known to affect fetal hemoglobin levels explains additional genetic
597 variation. *Nature genetics* 42, 1049.

598 13. Trynka, G., Hunt, K.A., Bockett, N.A., Romanos, J., Mistry, V., Szperl, A., Bakker, S.F., Bardella,
599 M.T., Bhaw-Rosun, L., and Castillejo, G. (2011). Dense genotyping identifies and localizes
600 multiple common and rare variant association signals in celiac disease. *Nature genetics* 43,
601 1193-1201.

602 14. Quintana, M.A., Schumacher, F.R., Casey, G., Bernstein, J.L., Li, L., and Conti, D.V. (2012).
603 Incorporating prior biologic information for high-dimensional rare variant association studies.
604 *Human heredity* 74, 184-195.

605 15. Quintana, M., and Conti, D. (2013). Integrative variable selection via Bayesian model
606 uncertainty. *Statistics in medicine* 32, 4938-4953.

607 16. Benner, C., Spencer, C.C., Havulinna, A.S., Salomaa, V., Ripatti, S., and Pirinen, M. (2016).
608 FINEMAP: efficient variable selection using summary data from genome-wide association
609 studies. *Bioinformatics* 32, 1493-1501.

610 17. Yang, J., Ferreira, T., Morris, A.P., Medland, S.E., Madden, P.A., Heath, A.C., Martin, N.G.,
611 Montgomery, G.W., Weedon, M.N., Loos, R.J., et al. (2012). Conditional and joint multiple-SNP
612 analysis of GWAS summary statistics identifies additional variants influencing complex traits. *Nat
613 Genet* 44, 369-375, S361-363. 10.1038/ng.2213.

614 18. Verzilli, C., Shah, T., Casas, J.P., Chapman, J., Sandhu, M., Debenham, S.L., Boekholdt, M.S.,
615 Khaw, K.T., Wareham, N.J., and Judson, R. (2008). Bayesian meta-analysis of genetic association
616 studies with different sets of markers. *The American Journal of Human Genetics* 82, 859-872.

617 19. Newcombe, P.J., Conti, D.V., and Richardson, S. (2016). JAM: A Scalable Bayesian Framework for
618 Joint Analysis of Marginal SNP Effects. *Genet Epidemiol* 40, 188-201. 10.1002/gepi.21953.

619 20. Mahajan, A., Go, M.J., Zhang, W., Below, J.E., Gaulton, K.J., Ferreira, T., Horikoshi, M., Johnson,
620 A.D., Ng, M.C., and Prokopenko, I. (2014). Genome-wide trans-ancestry meta-analysis provides
621 insight into the genetic architecture of type 2 diabetes susceptibility. *Nature genetics* 46, 234-
622 244.

623 21. Conti, D.V., Darst, B.F., Moss, L.C., Saunders, E.J., Sheng, X., Chou, A., Schumacher, F.R., Al
624 Olama, A.A., Benlloch, S., and Dadaev, T. (2021). Trans-ancestry genome-wide association meta-
625 analysis of prostate cancer identifies new susceptibility loci and informs genetic risk prediction.
626 *Nature genetics* 53, 65-75.

627 22. Asimit, J.L., Hatzikotoulas, K., McCarthy, M., Morris, A.P., and Zeggini, E. (2016). Trans-ethnic
628 study design approaches for fine-mapping. *European journal of human genetics* 24, 1330-1336.

629 23. Kichaev, G., and Pasaniuc, B. (2015). Leveraging functional-annotation data in trans-ethnic fine-
630 mapping studies. *The American Journal of Human Genetics* 97, 260-271.

631 24. Teo, Y.Y., Ong, R.T., Sim, X., Tai, E.S., and Chia, K.S. (2010). Identifying candidate causal variants
632 via trans - population fine - mapping. *Genetic epidemiology* 34, 653-664.

633 25. Campbell, M.C., and Tishkoff, S.A. (2008). African genetic diversity: implications for human
634 demographic history, modern human origins, and complex disease mapping. *Annu. Rev.
635 Genomics Hum. Genet.* 9, 403-433.

636 26. Shi, H., Burch, K.S., Johnson, R., Freund, M.K., Kichaev, G., Mancuso, N., Manuel, A.M., Dong, N.,
637 and Pasaniuc, B. (2020). Localizing Components of Shared Transetnic Genetic Architecture of
638 Complex Traits from GWAS Summary Data. *The American Journal of Human Genetics* 106, 805-
639 817. 10.1016/j.ajhg.2020.04.012.

640 27. Zanetti, D., and Weale, M.E. (2018). Transethnic differences in GWAS signals: A simulation study.
641 Annals of Human Genetics 82, 280-286. 10.1111/ahg.12251.

642 28. Marigorta, U.M., and Navarro, A. (2013). High Trans-ethnic Replicability of GWAS Results Implies
643 Common Causal Variants. PLoS Genetics 9, e1003566. 10.1371/journal.pgen.1003566.

644 29. Hu, Y., Tanaka, T., Zhu, J., Guan, W., Wu, J.H., Psaty, B.M., McKnight, B., King, I.B., Sun, Q., and
645 Richard, M. (2017). Discovery and fine-mapping of loci associated with MUFAs through trans-
646 ethnic meta-analysis in Chinese and European populations. Journal of lipid research 58, 974-981.

647 30. Morris, A.P. (2011). Transethnic meta - analysis of genomewide association studies. Genetic
648 epidemiology 35, 809-822.

649 31. Lapierre, N., Taraszka, K., Huang, H., He, R., Hormozdiari, F., and Eskin, E. (2021). Identifying
650 causal variants by fine mapping across multiple studies. PLOS Genetics 17, e1009733.
10.1371/journal.pgen.1009733.

651 32. Yang, J., Ferreira, T., Morris, A.P., Medland, S.E., Madden, P.A.F., Heath, A.C., Martin, N.G.,
652 Montgomery, G.W., Weedon, M.N., Loos, R.J., et al. (2012). Conditional and joint multiple-SNP
653 analysis of GWAS summary statistics identifies additional variants influencing complex traits.
654 Nature Genetics 44, 369-375. 10.1038/ng.2213.

655 33. Goel, P., and Zellner, A. (1986). On assessing prior distributions and Bayesian regression analysis
656 with g-prior distributions. In Bayesian inference and decision techniques: Essays in Honor of
657 Bruno De Finetti, pp. 233-243.

658 34. Robins, J.M., and Greenland, S. (1992). Identifiability and exchangeability for direct and indirect
659 effects. Epidemiology 3, 143-155. 10.1097/00001648-199203000-00013.

660 35. Wang, G., Sarkar, A., Carbonetto, P., and Stephens, M. (2020). A simple new approach to
661 variable selection in regression, with application to genetic fine mapping. Journal of the Royal
662 Statistical Society Series B-Statistical Methodology 82, 1273-1300. 10.1111/rssb.12388.

663 36. Jiang, Y., Chen, S., McGuire, D., Chen, F., Liu, M., Iacono, W.G., Hewitt, J.K., Hokanson, J.E.,
664 Krauter, K., Laakso, M., et al. (2018). Proper conditional analysis in the presence of missing data:
665 Application to large scale meta-analysis of tobacco use phenotypes. PLOS Genetics 14,
666 e1007452. 10.1371/journal.pgen.1007452.

667 37. Wang, A., Shen, J., Rodriguez, A., Saunders, E., Chen, F., Darst, B., Sheng, X., Xu, Y., Chou, A.,
668 Benlloch, S., et al. (2022). Improving prostate cancer risk prediction through multi-ancestry
669 genome-wide discovery of 187 novel risk variants. [Manuscript submitted for publication].

670 38. Mahajan, A., Rodan, R., Aylin, Le, H., Thu, Gaulton, J., Kyle, Haessler, J., Stilp, M., Adrienne,
671 Kamatani, Y., Zhu, G., Sofer, T., Puri, S., et al. (2016). Trans-ethnic Fine Mapping Highlights
672 Kidney-Function Genes Linked to Salt Sensitivity. The American Journal of Human Genetics 99,
673 636-646. 10.1016/j.ajhg.2016.07.012.

674 39. Mahajan, A., Spracklen, C.N., Zhang, W., Ng, M.C.Y., Petty, L.E., Kitajima, H., Yu, G.Z., Rüeger, S.,
675 Speidel, L., Kim, Y.J., et al. (2022). Multi-ancestry genetic study of type 2 diabetes highlights the
676 power of diverse populations for discovery and translation. Nature Genetics 54, 560-572.
677 10.1038/s41588-022-01058-3.

678 40. Jiang, L., Xu, S., Mancuso, N., Newcombe, P.J., and Conti, D.V. (2021). A Hierarchical Approach
679 Using Marginal Summary Statistics for Multiple Intermediates in a Mendelian Randomization or
680 Transcriptome Analysis. Am J Epidemiol 190, 1148-1158. 10.1093/aje/kwaa287.

681 41. Benner, C., Havulinna, A.S., Järvelin, M.-R., Salomaa, V., Ripatti, S., and Pirinen, M. (2017).
682 Prospects of Fine-Mapping Trait-Associated Genomic Regions by Using Summary Statistics from
683 Genome-wide Association Studies. The American Journal of Human Genetics 101, 539-551.
684 10.1016/j.ajhg.2017.08.012.

685 42. Peterson, R.E., Kuchenbaecker, K., Walters, R.K., Chen, C.-Y., Popejoy, A.B., Periyasamy, S., Lam,
686 M., Iyegbe, C., Strawbridge, R.J., Brick, L., et al. (2019). Genome-wide Association Studies in
687

688 Ancestrally Diverse Populations: Opportunities, Methods, Pitfalls, and Recommendations. *Cell*
689 179, 589-603. 10.1016/j.cell.2019.08.051.
690 43. Li, B., and Ritchie, M. (2021). From GWAS to Gene: Transcriptome-Wide Association Studies and
691 Other Methods to Functionally Understand GWAS Discoveries. *Frontiers in Genetics* 12.
692 10.3389/fgene.2021.713230.
693

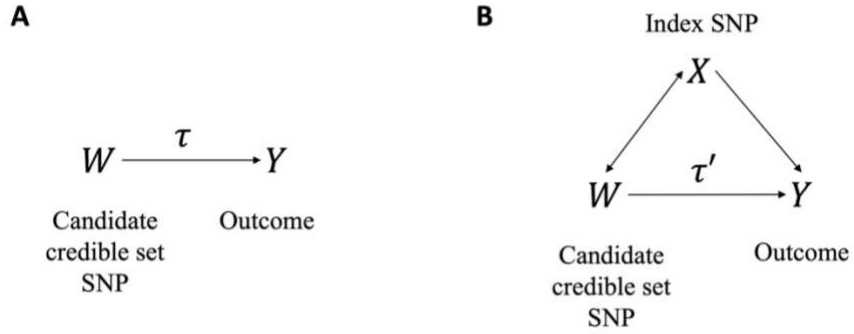


Figure 1 The direct acyclic graphs (DAG) for the probability that the index SNP mediates the candidate credible set SNP effect.

(A) *Model with the candidate credible set SNP, W , by itself. τ is the total effect of W on Y .* (B) *Model with W and X , the index SNP. τ' is the direct effect of W on Y .*

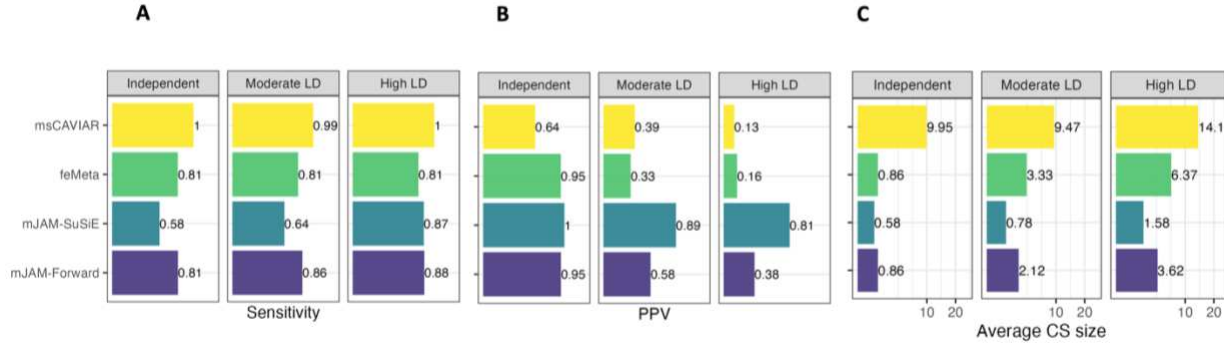


Figure 2 Credible set performance in simulation studies with artificial LD structure.

(A) *Sensitivity*, i.e. the proportion of 500 simulations where the true causal SNP was selected in a credible set. (B) *Positive Predictive Value (PPV)*, i.e., the proportion of true causal SNP over the credible set size, averaged over 500 iterations. (C) *Average CS size*.

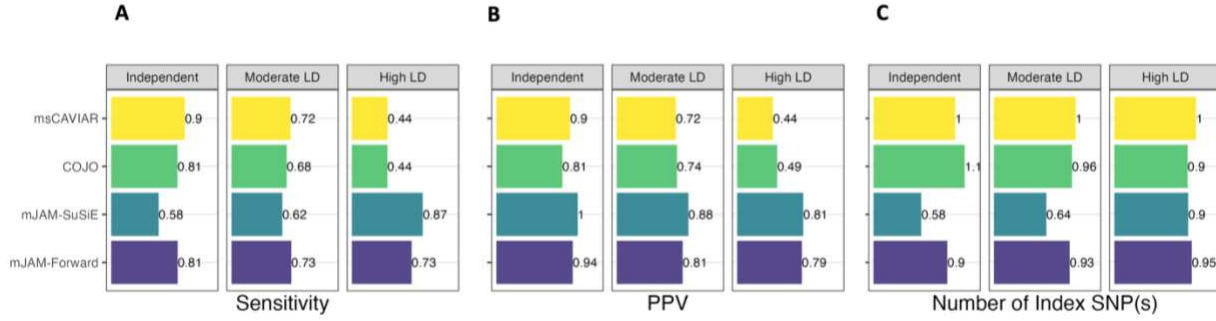


Figure 3 Performance of index SNP(s) selection in simulation studies with artificial LD structure.

(A) *Sensitivity*, i.e. the proportion of 500 simulations where the true causal SNP was selected in an index SNP. (B) *Positive Predictive Value (PPV)*, i.e., the proportion of causal SNP selected as an index over all selected indices, averaged over 500 iterations. (C) *Number of index SNP(s) selected*, averaged over 500 iterations.

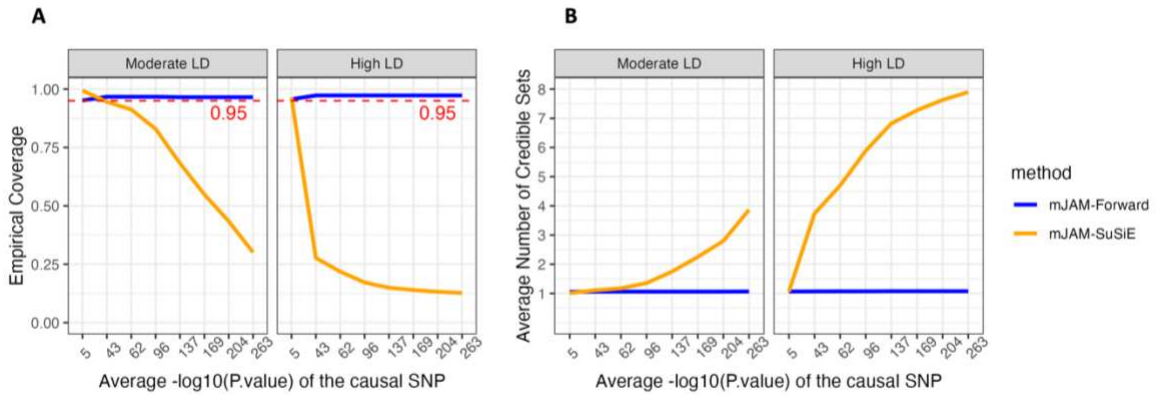


Figure 4 Credible set behaviour of mJAM-SuSiE and mJAM-Forward as causal SNP significance increases.

Simulations were conducted under baseline scenario setting (1 causal SNP out of 50 SNPs in total which are divided into 5 LD blocks) with varying effect sizes. The average empirical $-\log_{10}(P\text{-value})$ of the causal SNP ranged from 5 to 263, covering most situations seen in practice. Red dashed line indicates requested coverage which is set to be 0.95 for both methods. (A) Empirical credible set coverage; (B) Average number of credible sets selected among 500 simulations.

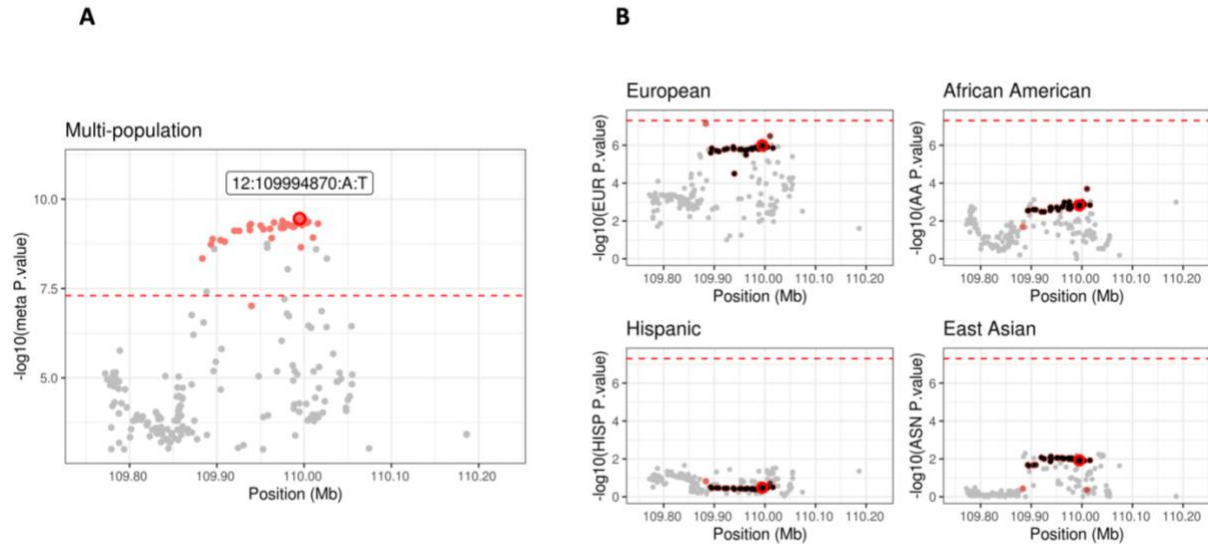


Figure 5 Manhattan plot for mJAM-Forward credible sets at chromosome 12 position

109194870 to 110794870.

(A) y-axis is meta-analyzed $-\log_{10}(P\text{-value})$ from multi-ethnic analysis; (B) y-axis is $-\log_{10}(P\text{-value})$ from ethnic-specific analysis.

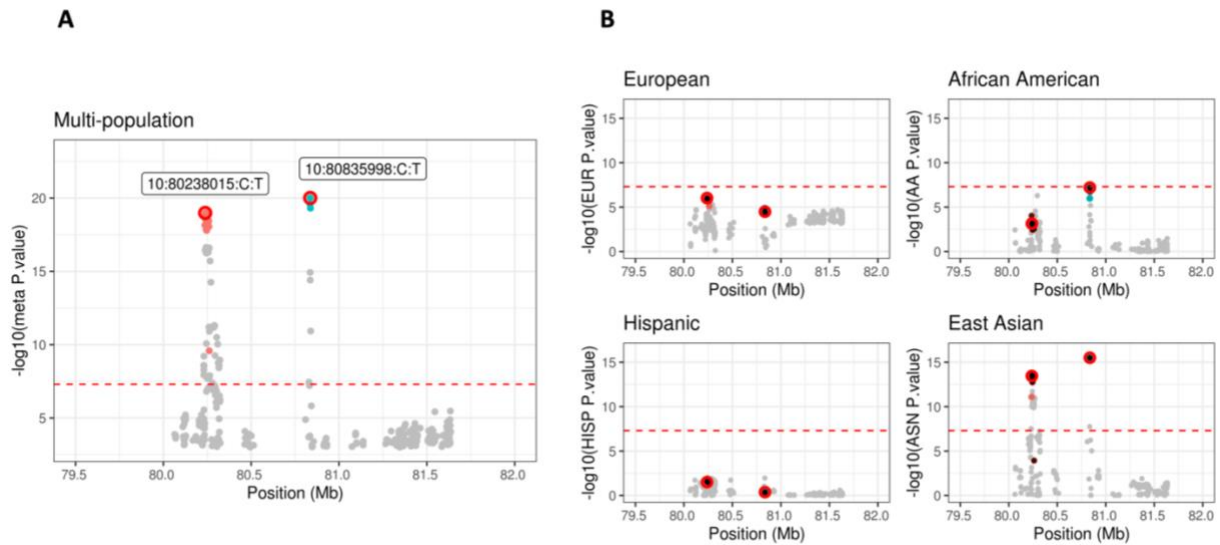


Figure 6 Manhattan plot for mJAM-Forward credible sets at chromosome 10 position

79436999 to 81635998.

(A) y -axis is meta-analyzed $-\log_{10}(P\text{-value})$ from multi-ethnic analysis; (B) y -axis is $-\log_{10}(P\text{-value})$ from ethnic-specific analysis.

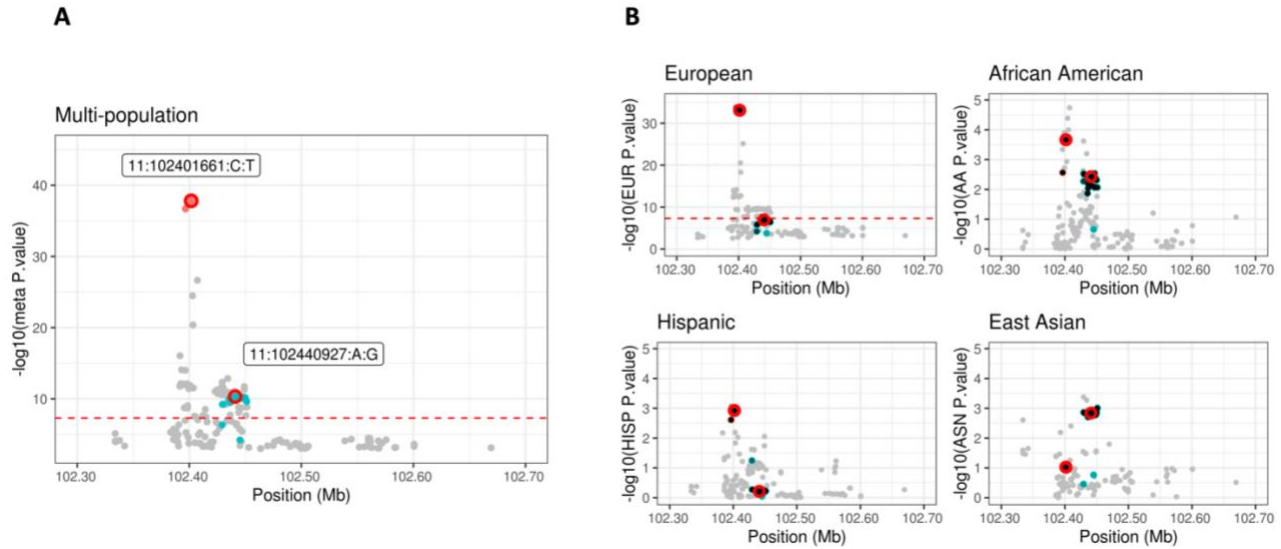


Figure 7 Manhattan plot for mJAM-Forward credible sets SNPs at chromosome 11

position 101601661 to 103201661.

(A) *y-axis is meta-analyzed $-\log_{10}(P\text{-value})$ from multi-ethnic analysis; (B) *y-axis is $-\log_{10}(P\text{-value})$ from ethnic-specific analysis.**